Development, Validation, and Practical Application of a Fast-Solving General-Purpose Thermal Analysis Tool – ONYX

Dr. Dean Schrage
dschrage@mainstream-engr.com
Mainstream Engineering Corporation
Rockledge FL 32955

Abstract

The evolution of modern computer-aided engineering (CAE) thermal analysis tools has produced software that is capable of extensive multidisciplinary simulations, featuring integrated computer-aided design (CAD) geometry, automated meshing, parametric modeling, topology optimization, etc. These tools are extremely capable but have two drawbacks. First, the large software architecture is costly, tending to limit license availability. Second, many first-order engineering thermal analysis problems do not warrant application of an extensive modern CAE toolset. The ONYX software fills this gap. The primary feature of the ONYX software is a simplified CAD foundation that utilizes quadrilateral (quad) geometry for the physical component representation. This represents a return to the heritage thermal software where geometry elements are equivalent to control volumes. This paper presents the layout of the ONYX software, describes the geometry construction, model equivalencing, conductance formulation, solution algorithms, and solution flow. We close the paper presenting a series of validations which reinforce the utility of sparse rapid control volume-based solvers.

Introduction

The design of the ONYX software stemmed from a practical problem that required numerous parametric simulations. We had explored the application of COMSOL to perform the analysis However, we showed that the CPU solution time required for a fully coupled fluid-thermal solution would prevent the full parametric trade space from being explored. As a tradeoff, we explored simplified one-dimensional (1D) analysis using MATLAB or Excel. However, we found that 1D treatments eliminated important spatial detail, complex geometry handling, graphical visualization and results-interpretation. From this, we began a focused development of a first-order general purpose thermal solver that would bridge extensive fully coupled solutions and simplified 1D domain representation.

Defining requirements, our original problem involved a 1) conjugate solid conduction, 2) natural convection exchange with the ambient fluid, coupling the solid components, 3) grey body surface-to-surface radiation exchange, and 4) rapid and stable transient solution. The original ONYX software was built around solving for a thermal network with these four features, ultimately satisfying the solution problem at hand. With time, the ONYX development has exceeded these original features, with adaptations to solve advection flow, and aeroheating, with other features yet planned.

Quad Elements

Early in the design phase, the quadrilateral (quad) was adopted as the primary element and continues to the present time. This was done for strategic reasons:

1. Quad elements represent a natural four-sided control volume (CV)
2. Quad elements take little memory to represent, process, and render
3. Quads can be subdivided into two triangles to compute surface normal and intersection logicals
4. Quad-quad connections can be processed for the conductance and advection matrices
5. Quad elements can be readily distorted to form any geometric shape

Figure 1 presents a working example of the quad utility in a solar heating problem. A hemisphere is solar heated, radiates and convects the ambient environment and interacts with the ground plane. A hemisphere geometry can be easily constructed with diminishing quads as shown, distorting to form the cap of the hemisphere. The direct solar heating regions and groundplane shaded regions are visible.

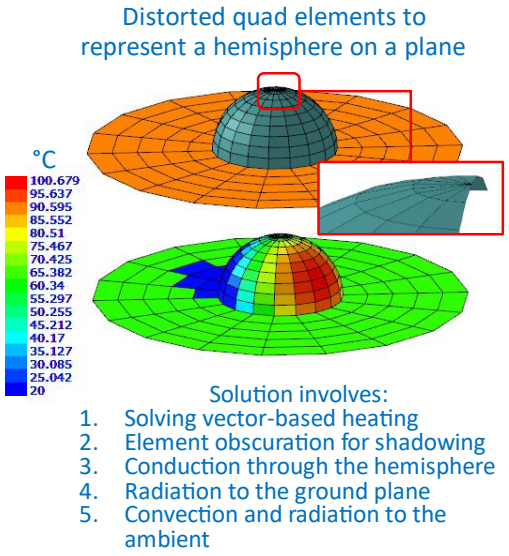

Figure 1. Solar heated hemisphere – quad construction.

Wavefront Neutral File

In ONYX, a neutral file interface is used to prepare geometry models for solution. This file is a modified *Wavefront* format, utilizing the standard facet-vertex formation, but with a custom color tag that references the property associated with the quad element. Figure 2 shows two elements extracted from the solar hemisphere model above. This figure shows the Wavefront definition of facets (f), vertices (v), and color (c) information. Any line of a free formatted Wavefront file can contain any of these designators. Typically, vertices are defined first, following by facets, followed by color. The Wavefront format is also dual-use supporting both pre- and post-processing. We summarize the key features of the Wavefront neutral file interface as follows:

1. Free formatted ASCII text model construction
2. Small model files that are human readable and easily modified
3. Three designators *v, f, c* to define a model
4. Color extension that allows the ONYX software to reference a property definition to each quad
5. 3D contour plots of models after solution, allowing smooth color progression to observe temperature gradients

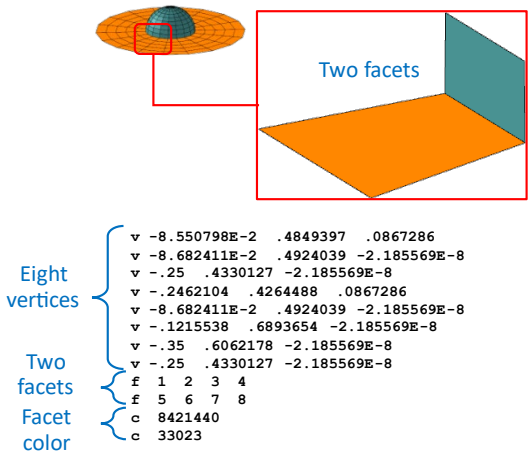

Figure 2. Modified Wavefront representation of geometry.

Quad to 3D Control Volume

Any thermal solver must represent three-dimensional (3D) elements to have any practical consideration. In ONYX, the quad element, having no rendered thickness, is extended to 3D by assigning a thickness in the color-referenced property. In this method, each quad has size definitions in the local quad coordinate system rst given by:

$$\Delta_{\boldsymbol{rst}} = \begin{bmatrix} \Delta_r \\ \Delta_s \\ \Delta_t \end{bmatrix}$$

The property defines element thickness Δ_t. The quad geometry is used to compute the sizes Δ_r and Δ_s. A virtual equivalent hexahedral is generated by each quad with thickness. This produces six flat faces to exchange energy across

Figure 3 shows a simple example of quad elements that curve to form a part of a cylinder. The in-plane unit vectors are always defined as $\boldsymbol{e_r}$ and $\boldsymbol{e_s}$ and the unit normal vector is $\boldsymbol{e_t}$. This figure shows the equivalent hexahedral.

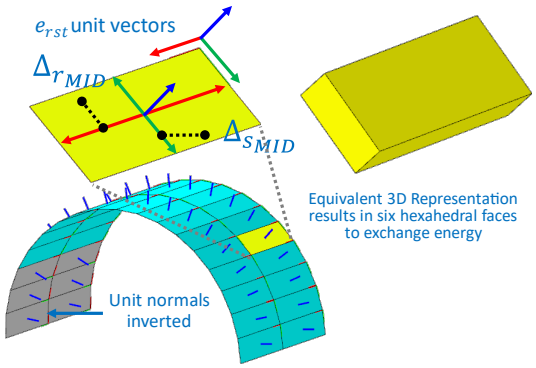

Figure 3. Equivalent 3D control volume and virtual hexahedral.

The quad grid sequencing, captured in the Wavefront neutral file, defines the unit normals. The user can roll grids to rotate $\boldsymbol{e_r}$ and $\boldsymbol{e_s}$ around the quad. Figure 3 shows grey colored elements with intentionally inverted unit normals. This feature is important when preparing models for surface-surface radiation and projected mesh connections.

To simplify the modeling for distorted elements, a modified element size is computed for Δ_r and Δ_s. This is done by solving for the area of a distorted quadrilateral and equating it to the area of the element defined by the mid-point average spans. A correction factor is solved that preserves the area of the quad. This is shown to work sufficiently well in the conductance modeling. Since it preserves area, heat loads defined by heat flux produce the correct, desired overall heat load on an element.

Equivalencing

The process of model equivalencing is the step where geometry elements are converted to control volume elements. Equivalencing is done in two steps:

1. Quad edge-to-edge equivalencing
2. Quad surface-to-surface equivalencing

The first compare quad edges to ensure that they are co-linear from both grid points to within a tolerance. The surface equivalencing is done with projected mesh connections and is only performed if the property of the quad calls for it. In both cases, any edge or surface that is detected as equivalenced with another surface produces logic that is used when forming the conductance matrices.

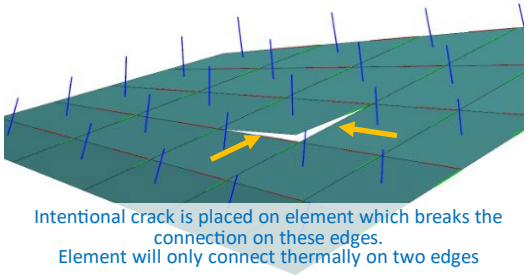

Figure 4. In-plane element equivalencing on coincident edges and intentional crack.

Edge Equivalencing

The ONYX software computes the rs-plane equivalencing in the pre-processing phase of modeling. Colinear quad edge lines defines the equivalencing in the $\boldsymbol{e_r}$ and $\boldsymbol{e_s}$ planes. Figure 4 illustrates in-plane element connections using edge equivalencing. An intentional crack is created by moving one vertex of the center quad. Since this quad only touches other quads on two edges, only two thermal connections are made.

The efficiency of quad edge equivalencing can be illustrated with a simple example of a ring fin. Figure 5 shows a very dense fin arrangement that is easily represented with single edge equivalencing. Any number of edge fins could be connected on the edge, provided they are rotated slightly to prevent equivalencing on the upper edges. This feature is used extensively in ONYX in order to test the addition of extended surface area to achieve desired component temperatures.

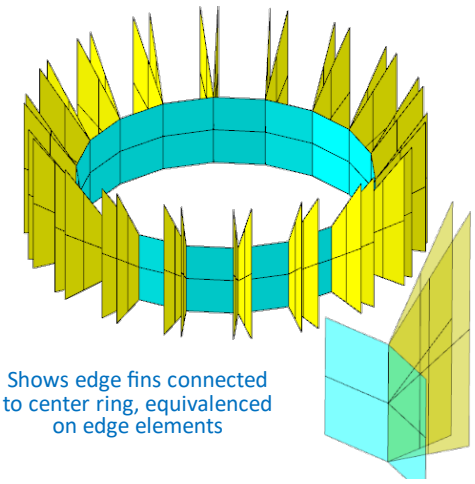

Figure 5. Quad edge connection efficiency example.

Surface Equivalencing

The $\boldsymbol{e_t}$ plane-normal equivalencing is determined with projected mesh couplings. This involves projecting normals to the nearest intersecting surface. The instructions for surface equivalencing are contained in the property in the form of unit normal projection directions. Any quad can connect to another quad by using a projected mesh coupling. A line-plane intersection algorithm is used to find all quads that can be potentially connected. The algorithm then selects the single closest projected quad and makes a connection. Figure 6 shows an application by connecting the edges of a cylinder to a disk. This does require additional quad elements to initiate the connection. These are shown dark red which form a projected connection to the green disk. This algorithm is also based on the shape factor algorithm and is partially dual-use. The ability to easily connect dissimilar meshes is one of the more important useful features on ONYX.

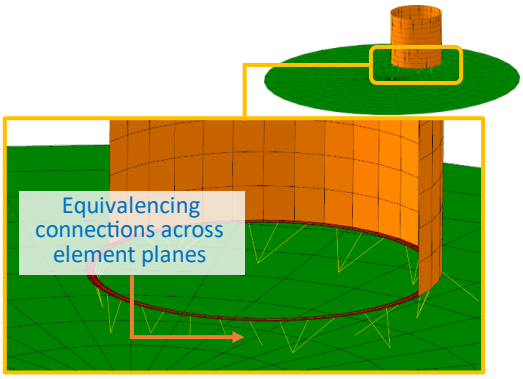

Shows projected mesh equivalencing that connects dissimilar mesh elements. These connections emanate from centroid of defined elements, pointing in the direction of the unit normal.

Figure 6. Surface equivalencing example used to connect dissimilar mesh elements.

Conservation Equation

An energy conservation equation is solved for all quad control volumes. Discretizing over all CV the compacted matrix equation for the temperature can be written:

$$\boldsymbol{C}\,\frac{d\boldsymbol{T}}{dt} = \boldsymbol{G}(\boldsymbol{T})\,\boldsymbol{T} + \boldsymbol{H}\,\boldsymbol{T} + \boldsymbol{S}$$

The bold terms signify vector and matrix terms and standard vector-matrix operations are applied.

Capacitance Term

The left side of the equation is the capacitance term, defined by the time-derivative of temperature and the capacitance matrix $\boldsymbol{C}$. The capacitance matrix is defined by density, volume and heat capacity:

$$\boldsymbol{C} = \rho\, \boldsymbol{V}\, C_p = \boldsymbol{m}\, C_p$$

This can be written as a function of the mass matrix mass matrix $\boldsymbol{m}$:

$$diag(\boldsymbol{m}) = [\rho_0 V_0 \quad \rho_1 V_1 \quad \rho_2 V_2 \quad \ldots]^T$$

Combined Conductance

The conductance matrix $\boldsymbol{G}(\boldsymbol{T})$ describes the combined conductance couplings between all control volumes. Considering just conduction in a solid for a constant conductivity, this term would be written in the more familiar form:

$$\boldsymbol{G_k} = k\, \boldsymbol{V}\, \nabla^2 \boldsymbol{T}$$

The term $\boldsymbol{V}$ is a diagonal matrix defined by the volume of the control volume.

The conductance matrix $\boldsymbol{G}(\boldsymbol{T})$ groups includes contributions from four terms:

1. Conduction couplings from edge-connected control volumes in the rs-plane
2. Conduction couplings from projection coupled control volumes in the quad normal direction $\boldsymbol{e_t}$
3. Convection couplings, both function-defined natural convection, and forced convection
4. Radiation couplings, both defined shape factor, and computed shape-factor derived

These are described in more detail in the section Conductance Models.

The matrix $\boldsymbol{G}(\boldsymbol{T})$ is shown as a function of the unknown temperature vector $\boldsymbol{T}$. Generally, the conduction couplings are weakly temperature dependent through variations in thermal properties. However, natural convection between elements is a function of temperature difference between elements. Similarly, the radiation conductance is a function of control volume temperature to the third power. This temperature dependence is addressed in the solution phase by performing updates during iterations and during specific time step increments.

Advection Conductance

The conductance matrix $\boldsymbol{H}$ describes the advection couplings that derive from elements which have a defined velocity and move energy in an out of the control volume by motion. For an incompressible substance, this term can be written:

$$\boldsymbol{H} = -\boldsymbol{C}\, \boldsymbol{u} \cdot \boldsymbol{\nabla}\, \boldsymbol{T}$$

Typically, this term is used to represent fluid advection in tubes. However, it is a generic advection term that can represent the transport of capacitive mass in the system from element flow. For example, a spinning disk brake that is friction heated has an advection term that derives from the spinning rotor carrying colder mass into the scrub surface.

Source Heating

The last term $\boldsymbol{S}$ is the source heating on each control volume. This is a property-defined value that is referenced to each control volume; it can include combinations of the following source components:

1. Fixed defined total control volume heat load
2. Fixed defined heat flux
3. Fixed defined volumetric heating
4. Variable vector-derived heat flux
5. Variable function-derived heat flux

The ONYX algorithm computes all possible contributions to each control volume. The

vector-derived and function-derived heat flux are updated on select refresh rates during transient solutions. For example, Figure 1 presented the transient solar heating of the hemisphere; in this case, the solar heat flux is computed every time step to account for variations in the sun's position.

Specific function references can be built into an ONYX property. Figure 7 shows an example of a steady-state solution of a laser-heated disk. In this example, the Gaussian heat flux profile is built into the property function. Passing the centroid of the control volume $\boldsymbol{c_{xyz}}$, the heat flux at any quad is determined relative to the beam centroid $\boldsymbol{r_{Beam.o}}$ as:

$$q''(r) = q''_{MAX}\, e^{\left(-\frac{r^2}{R_{1\sigma}{}^2}\right)}$$

$$r = \left|\boldsymbol{c_{xyz}} - \boldsymbol{r_{Beam.o}}\right|$$

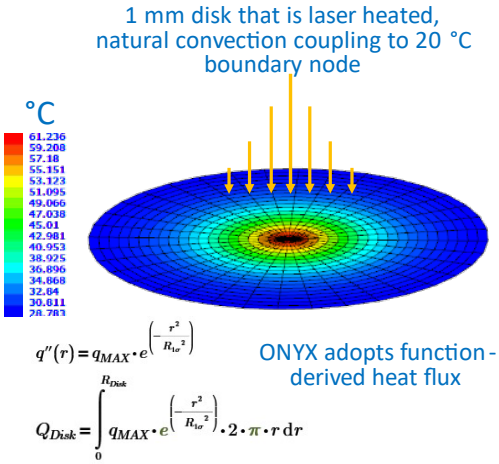

Figure 7. Laser heated disk with Gaussian heat flux profile

Solution Phase

Implicit Time Differencing

The ONYX solver uses implicit time differencing of the conservation equation described above. This ensures numerical stability but does require iteration at each time step. The above vectorized energy equation can be written as a function of discrete time level n as:

$$\boldsymbol{C}\,\frac{\boldsymbol{T}^{(n+1)} - \boldsymbol{T}^{(n)}}{\Delta t} = \boldsymbol{G}(\boldsymbol{T}^{(n+1)})\,\boldsymbol{T}^{(n+1)} + \boldsymbol{H}\,\boldsymbol{T}^{(n+1)} + \boldsymbol{S}$$

The differencing is implicit because the future-time temperature $\boldsymbol{T}^{(n+1)}$ appears on both sides of the equation. This would require a matrix inversion to solve directly. As will be showed, the equation is solved iterative which essentially performs incremental matrix inversion.

Steady-State Solution

Under steady-state conditions, we can solve the above equation by setting the capacitive term on the left side to zero. Adopting k as an iteration index, we can write a steady-state energy residual vector $\boldsymbol{\phi_{SS}}$ as follows:

$$\boldsymbol{\phi_{SS}}(\boldsymbol{T}^{(k)}) = \left(\boldsymbol{G}(\boldsymbol{T}^{(k)}) + \boldsymbol{H}\right)\boldsymbol{T}^{(k)} + \boldsymbol{S}$$

Applying a diagonalized Generalized Newton's (GN) method with successive over relaxation (SOR) factor ω_{SOR}, we can solve for the next temperature iteration at $k+1$ as:

$$\boldsymbol{T}^{(k+1)} = \boldsymbol{T}^{(k)} - \omega_{SOR}\left(\frac{\boldsymbol{\partial\phi}(\boldsymbol{T}^{(k)})}{\boldsymbol{\partial T}}\right)^{-1}\boldsymbol{\phi}^{(k)}$$

In the GN method, the term $\left(\frac{\boldsymbol{\partial\phi}(\boldsymbol{T}^{(k)})}{\boldsymbol{\partial T}}\right)^{-1}$ is a sparse matrix but generally diagonally dominant. It is simplified to a diagonal matrix so that its inverse is simply the inverse of the individual diagonal elements. The gradient is evaluated numerically by applying a small temperature change to the residual function:

$$\frac{\boldsymbol{\partial\phi}(\boldsymbol{T}^{(k)})}{\boldsymbol{\partial T}} \approx \frac{\boldsymbol{\phi}\left(\boldsymbol{T}^{(k)}\right) - \boldsymbol{\phi}(\boldsymbol{T}^{(k)} + \Delta\boldsymbol{T})}{\Delta\boldsymbol{T}}$$

The iteration proceeds until the energy imbalance is below a desired limit. The ONYX

solver computes the summation of absolute residuals ${\phi_{ABS.SUM}}^{(k)}$ to derive that measure:

$$ {\phi_{ABS.SUM}}^{(k)} = \sum_{i=0}^{N_{CV}-1} \left|\boldsymbol{\phi}_i^{(k)}\right| $$

The solver terminates when ${\phi_{ABS.SUM}}^{(k)} \leq 0.1\ W$. The termination criteria $0.1\ W$ is general and can be adjusted. Using this simplified SOR method, most thermal problems converge in about 1000 iterations.

Transient Solution

The methods presented for the steady state solution are readily adopted to the transient solution. The only change is the residual vector. Rewriting the time discretization equation, the transient energy residual vector $\boldsymbol{\phi_{TR}}$ can be written:

$$ \boldsymbol{\phi_{TR}}\left(\boldsymbol{T}^{(n+1,k)}\right) = \left(\boldsymbol{G}(\boldsymbol{T}^{(k)}) + \boldsymbol{H}\right)\boldsymbol{T}^{(n+1,k)} + \boldsymbol{S} - \boldsymbol{C}\,\frac{\boldsymbol{T}^{(n+1,k)} - \boldsymbol{T}^{(n)}}{\Delta t} $$

Or in a more compacted form, the transient residual is the steady state residual minus the capacitance term:

$$ \boldsymbol{\phi_{TR}}\left(\boldsymbol{T}^{(n+1,k)}\right) = \boldsymbol{\phi_{SS}}\left(\boldsymbol{T}^{(n+1,k)}\right) - \boldsymbol{C}\,\frac{\boldsymbol{T}^{(n+1,k)} - \boldsymbol{T}^{(n)}}{\Delta t} $$

This revised residual function is adopted in the GN solver at each time step. Using the past-time temperature vector $\boldsymbol{T}^{(n)}$, future time temperature $\boldsymbol{T}^{(n+1)}$ is computed iteratively using the Generalized Newton's algorithm outlined above. Essentially, each transient time step looks like a steady-state solution with a variable capacitive source term.

Validation Examples

The critical nature of software validation cannot be overstated. To this end, ONYX has been extensively validated, revealing many code deficiencies that have since been corrected. We present a small collection of our validation cases. We also conduct *soft-validation* by making code-to-code comparisons for specific test cases. This would be valid if the comparison code were a truth source. However, all software codes have flaws and it is possible the errors are simply repeated. In any event, our confidence in code integrity allows us to move to more complex problems.

Experimental Validations

Figure 8 presents a combined natural convection and radiation test case. The test data and images were taken from the SolariaThermal product page [1] with permission. The model is solved to steady state. The maximum IR camera measured temperature was 46.4 °C which compares closely the ONYX maximum of 47.3 °C.

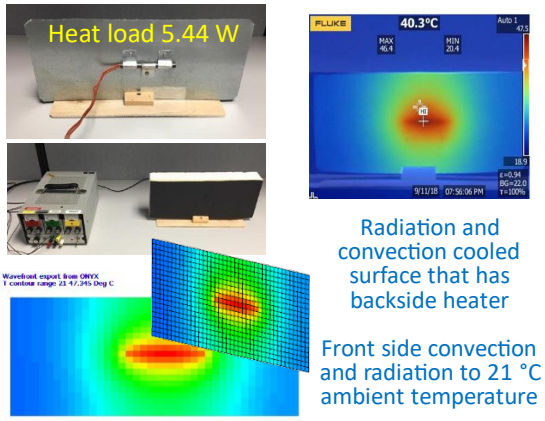

Figure 8. Validation case, natural convection and radiation cooled surface.

Figure 9 presents an aeroheating prediction of a two-stage biconic sounding rocket. Rumsey et al. [2] presented transient temperatures at various stations along the vehicle. Applying the trajectory, defined by altitude and velocity, a transient ONYX simulation was conducted that matched very closely. This utilized the aeroheating adaptation that is discussed in more detail below.

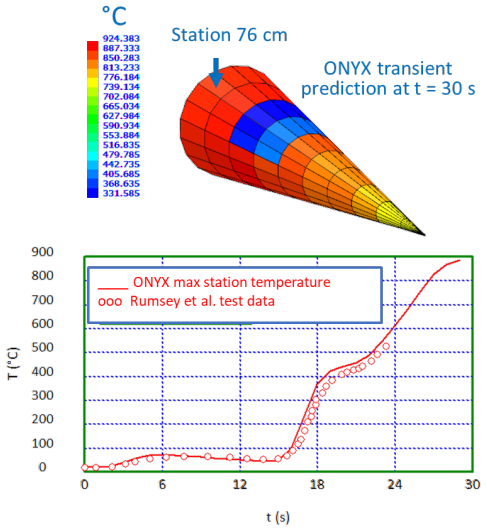

Figure 9. Validation case, two-stage biconic aeroheating.

Code-Code Validations

The following model comparisons are completely generic with no external reference. The comparison commercial codes are SolariaThermal [1] and COMSOL Multiphysics [3].

Figure 10 presents a comparison of a fin bank that has a backside heater. The maximum ONYX and COMSOL model temperatures differ by 20 °C, nominally 7% different based on the driving temperature difference.

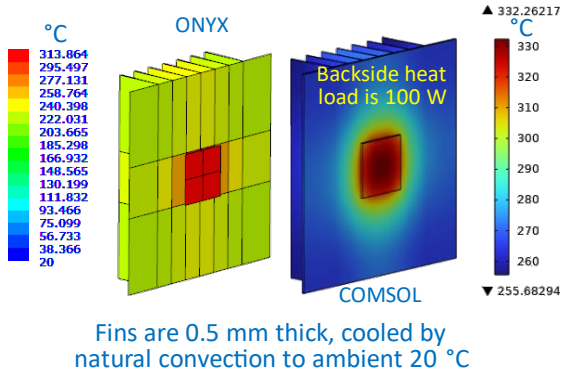

Figure 10. Fin bank with backside heater, natural convection cooled.

Figure 11 presents a comparison of surface-surface radiation where a sphere is heated at 100 W and radiates to adjacent walls. All surfaces have an emissivity of $\varepsilon = 0.9$. The walls are 2 mm thick Al 6061. One wall in the x-direction is attached to a 20 °C temperature boundary condition. The maximum ONYX and COMSOL models agree to with 9 °C, nominally 4% different based on the driving temperature difference.

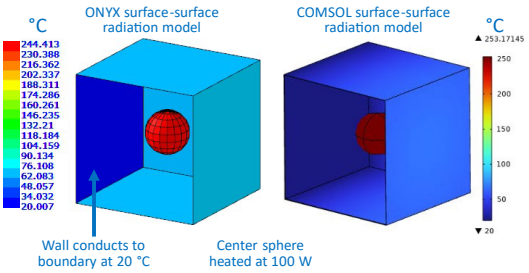

Figure 11. Surface-surface radiation test case.

Special Adaptations

This section describes two recent adaptations in ONYX that were developed to solve specific problems.

Advection Flows

The advection flow conductance matrix is constructed in ONYX. The quad is ideal to describe flows with defined advective velocity. The rs plane defines the area of flow passage and the property-defined thickness completes the 3D hexahedral flow passage. This is sufficient for modeling tube flow that moves energy around loops. The key feature is the application of windward or upwind differencing to describe $\boldsymbol{u} \cdot \boldsymbol{\nabla T}$. The ONYX code determines the upwind control volume when computing this term. The remaining advection conductance is described by the mass flowrate, specific heat:

$$G_{FL_{e_n}} = \boldsymbol{m_t} C_p \cdot \boldsymbol{e_n}$$

In this equation, the direction $\boldsymbol{e_n}$is limited to in-plane flows, i.e., $\boldsymbol{e_r}, \boldsymbol{e_s}$.

Aeroheating

Aeroheating is predicted by converting specific boundary quads to adiabatic wall nodes. These nodes have property definitions that carry an imbedded trajectory. This is used to compute the adiabatic wall temperature:

$$T_{AW} = T_{ATM} + r(Re_x, Pr)\,(T_x - T_{ATM})$$

$$T_x = T_{ATM} + \frac{1}{2}\frac{{V_x}^2}{C_p(T_{ATM})}$$

A reference temperature is defined using the adiabatic wall, atmospheric temperature, and the unknown quad wall temperature:

$$T_{REF} = T_{ATM} + 0.5\,(T_W - T_{ATM}) + 0.22\,(T_{AW} - T_{ATM})$$

This reference temperature is used to evaluate the thermal properties in the Nusselt correlation and Prandtl number.

The aeroheating prediction applies the local x station of the solid surface to compute an x-dependent Reynolds number Re_x. Using this value, along with a property reference temperature T_{REF}, the Nusselt number is predicted as a function of determined coefficients (a, b, and c), along with the Prandtl number Pr and the x-station defined Reynolds number Re_x according to:

$$Nu_x = a\,{Re_x}^b Pr^c$$

The local heat transfer coefficient is computed:

$$h_{CV}(x) = Nu_x \frac{k(T_{REF})}{x}$$

Because this varies over the station coordinate, an integrated average heat transfer coefficient is derived:

$$h_{CV_{AVG}}(x_o, L_{STA}) = \frac{1}{L_{STA}} \int_{x_o}^{x_o + L_{STA}} h_{CV}(x)\,dx$$

This average heat transfer coefficient is computed in the ONYX transient simulation by using the quad centroid to define the station x and the quad size span to define $L_{STA} = \Delta_r$.

Conclusions

The present paper describes a general purpose thermal analysis software that applies a common geometry and control volume thermal as a means to achieving efficient, fast model construction, and solution. This approach is a departure from the current modern CAE multidisciplinary toolset that employ body fitted meshing from geometry models. Despite the simplicity of the approach, the validations of the ONYX tool applied to practical engineering problems gives confidence in the solution approach and extension of the ONYX toolset to more sophisticated problems. It reinforces the notion that fast first-order solutions to most engineering problems are sufficient to support preliminary design scoping.

References

1. Internet images, used with permission, derived from https://www.solariathermal.com/ThermalTestCorrelation.html.
2. Rumsey, Charles B. and Lee, Dorothy B., Langley, October 15, 1956, Measurements Of Aerodynamic Heat Transfer and Boundary - Layer Transition On A 15 Degree Cone In Free Flight At Supersonic Mach Numbers Up To 5.2, Report Number RM L56F26, Aeronautical Laboratory Langley Field, Va., https://ntrs.nasa.gov/api/citations/19930089362/downloads/19930089362.pdf.
3. COMSOL Multiphysics Simulation Software, https://www.comsol.com/.

Appendices

Conductance Models

This section presents the formulations for the conductance models that are used to formulate the conductance matrix.

Conduction Conductance

The material conduction conductance is computed using the cross sectional area and conduction length. The half-conductance $G_{k_{e_n}}$ from the control surface of the virtual hexahedral to the centroid is defined by the face area $\boldsymbol{A} \cdot \boldsymbol{e_n}$ and the conduction distance $\frac{1}{2}\Delta_{\boldsymbol{rst}} \cdot \boldsymbol{e_n}$ and the thermal conductivity in that direction $\boldsymbol{k} \cdot \boldsymbol{e_n}$:

$$G_{k_{e_n}} = \boldsymbol{k} \cdot \boldsymbol{e_n} \frac{\boldsymbol{A} \cdot \boldsymbol{e_n}}{1/2\,\Delta_{\boldsymbol{rst}} \cdot \boldsymbol{e_n}}$$

In this formulation, $\boldsymbol{k}$ is the anisotropic conductivity vector in the rst directions. This half-conductance component is combined with likewise half terms when control volumes equivalence on edges or in planes. This conductance is also added in series when adopting convection or radiation conductance to adjoining quads.

Convection Conductance

The convection conductance $G_{CV_{e_n}}$ is simply the project of the computed convection heat transfer coefficient h_{CV} and the virtual hexahedral surface area projected in the $\boldsymbol{e_t}$ direction:

$$G_{CV_{e_n}} = h_{CV}\, \boldsymbol{A} \cdot \boldsymbol{e_t}$$

Radiation Conductance

The radiation conductance $G_{RA_{i,j}}$ between quads i and j is defined by the respective temperatures, emissivities, areas, and shape factor matrix $\boldsymbol{F}$:

$$G_{RA_{i,j}} = \sigma \frac{\left(T_i + T_j\right)\left({T_i}^2 + {T_j}^2\right)}{\frac{1}{A_{RA_i}}\left(\frac{1}{\varepsilon_i} - 1\right) + \frac{1}{A_{RA_j}}\left(\frac{1}{\varepsilon_j} - 1\right) + \frac{1}{A_{RA_i}\boldsymbol{F}_{i,j}}}$$

$$A_{RA_i} = \boldsymbol{A} \cdot \boldsymbol{e_{t_i}}$$

$$A_{RA_j} = \boldsymbol{A} \cdot \boldsymbol{e_{t_j}}$$

For quad that represent boundary conditions at fixed temperature, the projected area is assumed to be infinite. This equation is then simplified:

$$G_{RA_{i,j}} = \sigma\, \varepsilon_i\, A_{RA_i}\, F_{DEF_i} \left(T_i + T_j\right)\left({T_i}^2 + {T_j}^2\right)$$

The user can adopt a user-defined shape factor F_{DEF_i} to reduce this conductance value. Note this formulation is not a true grey-body view factor prediction, but it is sufficiently accurate for materials with an emissivity $\varepsilon \geq 0.5$.

Shape Factor Modeling

The radiation shape factor matrix $\boldsymbol{F}$ is computed for all property-defined participating quads in a model. The property specifies which surface is radiating with three options: 1) neither side, 2) normal positive side, 3) both sides. The shape factor matrix is computed by converting the continuous double integral to a discrete double integral over the quad surface. The continuous

integral for shape factor from quads i and j is described by:

$$F_{ij} = \frac{1}{A_i} \int \int \frac{\cos(\theta_i) \cos(\theta_j)}{\pi r_{ij}} dA_i dA_j$$

Figure 12 shows the angles that are presented by quads when making this calculation. Each quad in ONYX has a computed surface normal that is used in this angle calculation. The surfaces are subdivided to perform the double integral described above. The integration is one of the lengthier computations in ONYX during model pre-processing. In particular, the ONYX algorithms include obscuration analysis to determine if the vector r_{ij} is obscured by other model geometry. Overall, the direct integration method is not the fastest method to derive the shape factor, but it is relatively simple to program and debug.

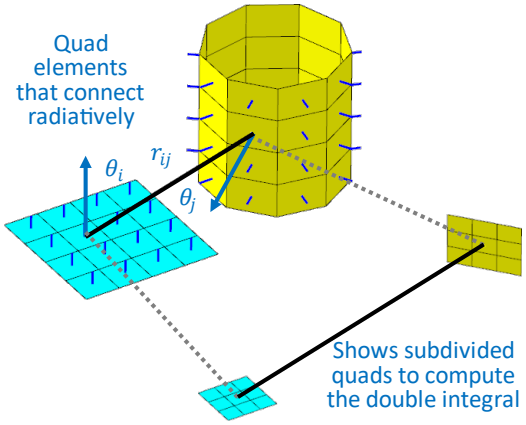

Figure 12. Shape factor modeling showing quad connection and area integration.